Looped Thermoacoustic Cryocooler with Self-Circulating Large Area Cooling

Thomas W. Steiner

Etalim Inc.
Burnaby, BC, V5J-5K4, Canada

ABSTRACT

A self-circulating loop replaces the expansion heat exchanger as an extension to a previously discussed 490 Hz thermoacoustic cryocooler design. A self-circulating loop allows for large area cooling without requiring long-distance thermal conduction. Instead, heat is transported by a steady flow of the working gas around a loop. Acoustic power directly provides the driving pressure for the circulation without requiring any moving parts and can work at low temperatures. A venturi mechanism previously proven in a thermoacoustic waste heat recovery engine provides the driving pressure. Modeling a proposed system using thermoacoustic theory shows that the acoustic power dissipated driving the loop can be less than what would otherwise be dissipated in an expansion heat exchanger. Thus large area cooling is possible with no loss of cooling capacity. The high frequency of operation enables a compact machine that is low cost and ultra-reliable.

INTRODUCTION

Regenerative cryocoolers have enjoyed commercial success in several applications [1]. However, they are not inherently endowed with the ability to cool a remote cooling load. They are restricted to local cooling loads within the range of solid conduction to the cryocooler cold finger. There are applications such as cryogenic propellant storage that require extensive surface area cooling and are thus problematic to cool with a regenerative cryocooler. Two groups have recently proposed solutions that couple a regenerative cryocooler and a separate circulating loop of cooled working gas to cool remote distributed loads [2,3]. The circulating loop is driven by a separate compressor, either at ambient temperature but isolated from the cryogenic zone by a pulse tube [2], or with the compressor itself operating at cryogenic temperature [3]. Both of these solutions employ reed valves at cryogenic temperatures.

A high-frequency (490 Hz) thermoacoustic (TA) cryocooler was recently proposed as an alternative to pulse tube or Stirling cryocoolers for the intermediate temperature range (>50 K) [4]. The high operating frequency is key to making a pure flexure-based cryocooler without any sliding components or valves. Such a cryocooler can achieve good performance, high specific power, and ultra-long life at a low cost. An optimized version of such a cryocooler with bespoke parts suitable for cryogenic temperatures has not yet been built, but a first test using available, but inherently unsuitable thermoacoustic engine parts has nevertheless achieved a temperature of 140 K.

Cryocoolers 22, edited by R.G. Ross, Jr., J.R. Raab and S.D. Miller

With 490 Hz operation and helium as the working gas, the wavelength of sound is about 2.1 m at ambient temperature and 1.05 m at 77 K. At this frequency, tuned half or quarter wavelength ducts are conveniently short and have low acoustic losses. Short ducts allow for a relatively compact and efficient looped thermoacoustic apparatus. An intriguing possibility is adding a pair of additional quarter wavelength ducts coupled to low pass filter volumes to build a self-circulating loop. This loop is driven by acoustic power alone and can cool a distributed load without requiring a secondary compressor or valves.

Furthermore, the self-circulating loop replaces the otherwise necessary expansion side heat exchanger. The acoustic power dissipated to drive the loop is less than the power otherwise dissipated in the expansion exchanger, so performance is improved. A TA cryocooler with distributed cooling and without a performance penalty is realistic. Furthermore, such a system provides distributed cooling without needing an additional compressor and associated components. It is thus a much simpler system with fewer possible points of failure. The self-circulating loop consists of nothing more than tubing and is likely lower cost than the heat exchanger otherwise needed. Drastic cost reduction of an ultra-reliable system suitable for cooling a distributed load is possible.

SELF-CIRCULATING LOOP

Using a self-circulating loop (SCL) for delivering heat to thermoacoustic devices was suggested by Swift and Backhaus [5]. Their proposed loops use an element with asymmetric minor losses to convert some acoustic power to static pressure. An alternative, lower loss method of driving such a loop is using the venturi effect [6]. This loop driving method successfully delivered heat to a waste heat recovery thermoacoustic engine [7]. The same principle will work even better at cryogenic temperatures due to the lower gas viscosity and higher density. It is straightforward to produce driving pressures around 10 kPa, and loop mass flows of 10 g/s without dissipating much acoustic power.

A schematic diagram of the operating principle is in Figure 1. The self-circulating loop proximal ends connect to the TA cryocooler on the regenerator's expansion side and replace the expansion heat exchanger. The duct ends are much less than a wavelength apart and see almost identical oscillating pressure amplitudes. However, one end is placed at a narrowing of the ducting (the

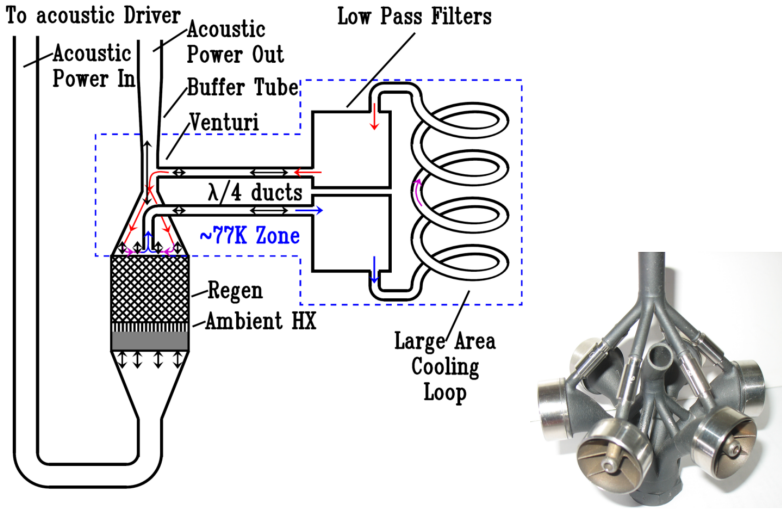

Figure 1. A not-to-scale schematic of the cryocooler head with a self-circulating loop for cooling a remote and extended area load. Acoustic oscillating flows are the double-headed black arrows while the superimposed small steady flow in the SCL is temperature color coded. Insert is an image of the expansion manifold with self-circulating loop as used in a waste heat recovery engine.

venturi) while the other faces the regenerator. The acoustic volumetric flow at both ends is almost identical, but the gas velocity is substantially larger at the venturi end. The velocity difference establishes a static pressure that drives a steady flow through the loop. This steady flow is superimposed on the acoustic flow at the expansion end of the regenerator. The working gas migrates over the regenerator surface substantially radially inward toward the SCL loop exit while oscillating in and out of the regenerator, where it is cooled.

A disadvantage of high-frequency operation is that an optimized regenerator needs a larger frontal area, smaller pore hydraulic radius, and shorter flow length than a regenerator in a lower frequency regenerative cryocooler. An optimized high-frequency machine has smaller duct than regenerator areas. Thus, a funnel structure is always necessary to couple the regenerator to the acoustic ducts, and a natural venturi zone exists without explicit narrowing. Little if any additional narrowing is needed to construct the venturi. The narrowed venturi zone produces hardly any additional acoustic losses other than losses associated with the T-junction to the SCL duct.

Figure 1 also shows an image of the expansion manifold used with a waste heat recovery thermoacoustic engine [7]. Front and center in the image are two of the six in-parallel regenerator interface heads showing proximal SCL return ducts at the centers. For this expansion manifold, with six in-parallel regenerators, the SCL loop ducts also branch into six smaller tubes at the expansion manifold ends. The in-parallel venturi ends are visible between the heads and lower down in the image. They connect to a single SCL duct bending out of the page toward the viewer. The six SCL return ducts combine into a larger SCL duct at the top of the image. A single buffer tube interface at the very bottom collects acoustic flow from all six heads.

The vanes in the heads assist in the acoustic power turning the corner smoothly. The turn was necessary for the waste heat recovery engine due to implementation-specific geometric constraints but is not a required feature for operation. The cryocooler modelled here also uses six in-parallel regenerators but does not have a 90-degree acoustic path turn in the manifold. Simulated cryocooler performance is very sensitive to the volume between the regenerators and the narrow expansion plenum ducting. A significant volume makes it difficult to achieve a sufficient magnitude reactive or standing wave contribution on the expansion side to minimize regenerator losses. Kotsubo [8] provides a good explanation of why it is necessary to have such a reactive flow superimposed on the travelling wave component. Thus, a large cone angle is appropriate to narrow the flow passages quickly. It is then advantageous to implement some system of vanes to reduce the rapid expansion local losses [9], although there will be a cost due to extra hysteresis losses on the extra surface area. A system of vanes will also help provide uniform acoustic flow to the expansion side of the regenerator and thereby reducing unwanted secondary flows.

A design goal is to minimize the acoustic power that flows into the SCL ducts, which are entirely within the cold zone. The cryocooler must lift any power dissipated in the SCL reducing the cooling power. Low acoustic power flow into the ducts is achieved by duct tuning so that the acoustic impedance at the openings is as large as possible. Making the length of the ducts a quarter wavelength at the operating frequency and temperature of the ducts achieves this goal. The tuned duct cross-sectional area also affects the parasitic power dissipation. Thus, the duct flow area should be no larger than what is necessary to support the desired steady flow.

The distal ends of the SCL ducts connect to volumes labeled low-pass filters in the schematic. These filters are nothing more than a length of much larger diameter tubing so that any acoustic flows into these volumes are insufficient to produce much pressure swing. These filters result in practically zero acoustic flow in the extended area cooling loop, which may thus be of arbitrary length and diameter. However, the length and diameter of the cooling loop affect the magnitude of the pressure drop associated with the steady flow. The amount of pressure the venturi needs to generate is thus dependent on the cooling loop design and the desired steady mass flow. Also, the loop diameter and length must be sufficient to provide enough surface area to transfer the load heat into the circulating working gas with a small temperature delta.

LOOP DRIVING PRESSURE

The driving pressure's origin is the high-velocity flow across the branch. The pressure does not depend on the trunk flow direction, as it is ultimately due to energy conservation. The acoustic reversible time-averaged pressure is given by [10]

$$p_{2,rev} = \frac{|p_1|^2}{4\rho_m a^2} - \frac{|u_1|^2}{4} \tag{1}$$

where $|p_1|$ is the oscillating pressure amplitude, ρ_m is the mean gas density, a is the sound speed, and $|u_1| = |U_1|/A$ is the velocity amplitude. If there is a difference in the $p_{2,rev}$ between the two duct ends Δp_2, then a steady streaming flow can be driven through the loop

$$U_2 = \frac{\Delta p_2}{R_{loop}} \tag{2}$$

where U_2 is the volumetric flow driven by a pressure difference Δp_2 through loop hydraulic resistance R_{loop}.

As the input and output ends of the SCL are close together, the pressure amplitude at both ends is practically identical, and there is thus no contribution from the first term in Equation 1 to Δp_2. The velocity amplitudes $|u_1|$ at the two ends of the SCL loop can be substantially different despite the near-identical pressure $|p_1|$ and volumetric flow $|U_1|$ amplitudes if the flow cross-section area A changes between SCL ends, as in Figure 1.

Equation 1 is the static pressure in the absence of induced steady flow ($U_2 = 0$). However, the loop driving pressure Δp_2 will drop if it drives a branch flow U_2. For non-zero U_2, the side branch pressure and the trunk flow pressure drop are determined from the hydraulic pressure drops of a T-branch as presented in a table by Idelchik [9]. Estimating the average pressure produced by taking a cycle average is reasonable and produces the same zero flow pressure as given by Equation 1. At every point in the cycle, the Δp_2 pressure corresponds to negative branch pressures in these tables, as it is a branch pressure gain at the expense of the trunk flow rather than a head loss. The developed branch pressure drops if this pressure drives a branch flow.

In Equation 2, Δp_2 is thus a function of U_2. Furthermore R_{loop} is also a function of U_2 if the steady flow is large enough to be turbulent, as will generally be the case. Thus, Equation 2 is non-linear, but is solvable by iteration.

The open-loop venturi pressure is proportional to the fluid density and the square of the trunk velocity past the opening. The mechanism thus produces a substantially larger pressure at cryogenic temperatures than at elevated temperatures for the same trunk flow velocity. Generating the loop driving pressure has a lower power dissipation cost in a cryogenic application than in a waste heat recovery application [7]. An additional benefit at cryogenic temperatures is that the extra density gives a correspondingly larger heat carrying capacity for a given U_2.

The graphs in Figure 2 are with a trunk flow amplitude of 10 *l*/s, a venturi trunk cross-sectional area of 300 mm^2, a side branch area of 38 mm^2, a helium working gas density of 50 kg/m^3 as determined for a temperature of 77 K, and pressure of 8 MPa. With the given trunk volumetric flow and area, the trunk velocity across the venturi has an amplitude of 33 m/s.

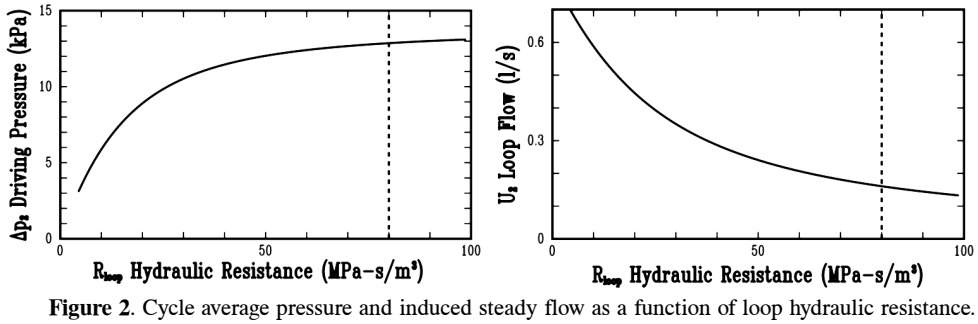

Figure 2. Cycle average pressure and induced steady flow as a function of loop hydraulic resistance. The extended area cooling loop usually dominates the loop hydraulic resistance. The dashed line indicates the SCL operating point in the simulated cryocooler.

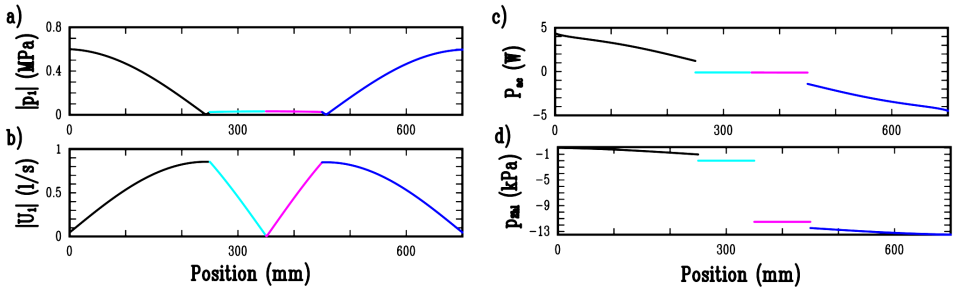

Figure 3. Acoustic model results for the self-circulating loop driven from both ends. Integration direction is left to right from the flow return open end at the left to the venturi opening at the right. Color changes correspond to different elements with the quarter wavelength ducts on the outside and the low pass filters in the center. The extended area cooling loop is modelled as a point resistance between the low pass filter volumes. Trunk flow, oscillating pressure amplitudes, and geometry are set to match the usage in a simulated cryocooler: a) the acoustic pressure amplitude, b) the volumetric flow amplitude, c) the acoustic power, d) head loss pressure due to steady flow.

SCL ACOUSTIC MODEL

The SCL acoustic simulation results are in Figure 3. The acoustic boundary conditions are similar pressure phasors at both ends. The pressure phasors in the expansion manifold are an output of a thermoacoustic model of the cryocooler and provide input to the SCL acoustic calculation. As seen in Figure 3a, the pressure amplitudes at the open endpoints of the loop in the expansion manifold are almost the same. The first (black) and last (blue) segments are the quarter wavelength ducts, while the cyan and magenta correspond to the low pass filters. There is practically no acoustic power flowing in the cooling loop, and it is inconveniently long to display on this graph. Thus, the cooling loop is modeled as a point resistance without spatial extent.

The driving pressure sets up standing waves in both SCL ducts as they are a quarter wavelength at the operating frequency. The pressure oscillations at the proximal ends transform into volumetric flow oscillations at the low pass filter ends, as seen in Figure 3b. Note that there is very little flow into the proximal ends when the ducts are tuned correctly. This corresponds to the desired high impedance state that minimizes the diversion of acoustic power into the SCL loop. Even when perfectly tuned, some parasitic acoustic power flows into the proximal ends (Figure 3c). This power is needed to overcome the acoustic dissipations in the SCL. Acoustic power flows in towards the filter volumes from both sides. It is negative on the right of Figure 3c as it flows against the integration direction. The duct diameters affect the parasitic power flowing into the ducts, the venturi pressure, the circulating mass flow, and the steady flow head loss. The SCL duct and cooling loop diameters must thus be chosen correctly for the scale of the device.

The step changes in flow and power between segments correspond to local loss segments without spatial extent. Local losses at the junctions between ducts and filter volumes are significant since the oscillating flows are relatively large at those locations. These transitions should have some rounding to minimize these losses. At the proximal ends, the flows are low enough that local acoustic losses are insignificant. However, local losses at the proximal ends may affect the steady flow head loss; thus, these transitions will also benefit from rounding.

The steady flow resistance of the SCL system, including the large area cooling loop, sets the circulating mass flow as per Equation 2. The mass flow will increase until the steady flow head loss matches the driving pressure. Figure 3d shows the calculated steady flow head loss with the significant step change at the center corresponding to the head loss for flow through the cooling loop here represented with a suitably sized point resistor corresponding to an equivalent actual resistance of a long tube of a given diameter and with turbulence taken into account. The turbulence means that it is not a fixed resistance but must be self-consistent with the steady mass flow. The diameter and length of the large area cooling loop will have almost no effect on the SCL acoustic flow but will affect the loop resistance. The cooling duct diameter may be increased as necessary to get a low enough steady flow resistance to achieve a desired circulating flow.

Ideally, the steady flow is larger than the oscillating flow into the proximal ends of the SCL ducts. In that case, there is no flow reversal at the openings, and the superimposed acoustic flow produces a minor oscillation in the uni-directional flow magnitude. No flow reversal simplifies the calculation of the venturi pressure, but the venturi will still work to some extent even if the flow reverses. Flow reversal is usually not a problem at the operating design point, but reversal can occur during start-up. At start-up, the entire apparatus is at ambient temperature, and since the sound velocity is temperature-dependent, the SCL ducts will be far from a quarter wavelength. In that case, the acoustic flows into the SCL ducts will be much larger and may exceed the steady flow, causing flow reversals. In addition, the parasitic acoustic power flow into the SCL ducts will also be much larger, but as the cryocooler's cooling power at higher temperatures will also be greater, it will not prevent the apparatus from cooling down provided the parasitic losses are less than the cooling power. The need to cool from ambient sets a practical limit on the SCL duct diameter and hence on the achievable steady mass flow. Using an SCL tuned for low-temperature operation will reduce cooling power at higher temperatures. An SCL will only be optimal at a given design temperature.

An SCL instead of a cold side heat exchanger is particularly advantageous when operating at high frequency as there is some acoustic leakage into the SCL. This leakage is needed to overcome acoustic losses in the tuned SCL ducts and scales with the length of the ducts. Thus, operation at 50 Hz instead of 500 Hz would require about 10x longer tuned ducts with about 10x more dissipation.

CRYOCOOLER THERMOACOUSTIC MODEL

Full simulation results of a concept cryocooler with an SCL are shown in Figure 4. Standard thermoacoustic methods are used [11,12]. The device's scale is set by reusing existing, proven engine parts. Thus, the cryocooler simulation uses six in-parallel regenerators in a conceptual arrangement similar to Figure 1, the waste heat recovery manifold. The acoustic driver in the simulation is the existing all-flexure driver [13,4], but with the outer chamber heights increased to provide the necessary compliance volume for this application.

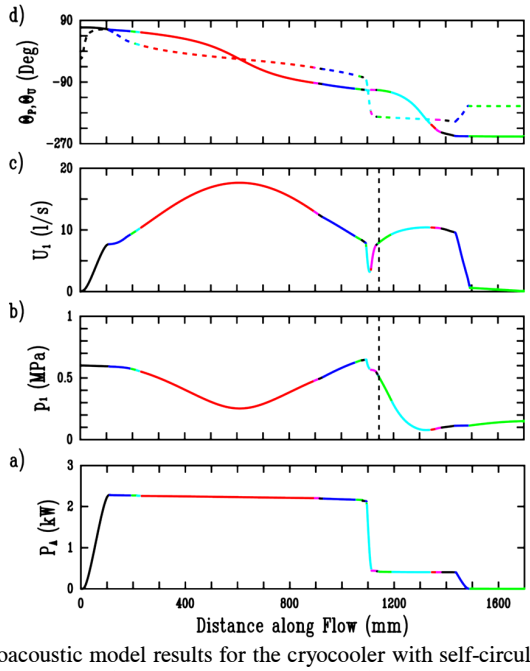

Figure 4. Thermoacoustic model results for the cryocooler with self-circulating loop. Color changes correspond to different elements in the model. a) the acoustic power b) the pressure amplitude c) the volumetric flow amplitude, d) pressure (solid) and flow (dashed) phases relative to the driver flexure motion. The vertical black dashed line in b) and c) is the location of the venturi side branch

The regenerators are of the same diameter as in the waste heat recovery engine, 30 mm, but the regenerator hydraulic radius (3.3 μm) and flow length (17 mm) were adjusted to be more optimum for cryogenic operation. For the cryocooler simulation, the regenerator was modelled as a glass microcapillary array rather than the rolled foil regenerators typically used in our engines for two reasons. First, such a regenerator can be fabricated from fused silica with the desired hydraulic radius, whereas with rolled foil, this hydraulic radius is challenging and untested. Second, the thermoacoustic theory of microcapillary arrays is very well understood [11], and hence the calculated total power in the regenerator will be reliable. The same cannot be said about foil regenerators with thermal breaks where the total power calculation is less certain. Since the cooling power is the difference between acoustic power out of the regenerator's cold side and the regenerator's total power, the calculated cooling power will then also be reliable.

The ambient side heat exchangers are the same as the proven engine exchangers using a flocked copper layer as the heat exchange layer [14]. The cold side heat exchangers have been replaced with the self-circulating loop as they are no longer required. The long cooling loop allows heat transfer into the working gas with very low heat flux and without space constraints. If desired, localized cooling can be enhanced by placing a more compact heat exchanger into the loop at one or more locations. Localized heat exchangers are also not space constrained. The only constraint is keeping the total loop pressure drop compatible with the venturi-generated driving pressure.

With the cryocooler target temperature set to 77 K, the duct lengths of the cryocooler and SCL were tuned accordingly. The self-circulating mass flow target was 10 g/s, corresponding to about 50 W/K of heat transport capacity with helium as the working gas. Then with 200 W of cooling power, the temperature difference between the input and output of the SCL is only 4 K. The inner radius of the 10 m long extended cooling loop duct was set to 4 mm to permit this steady flow with the available venturi pressure generated. The SCL quarter wavelength tuned ducts are 270 mm long and have a slightly smaller 3.5 mm radius. The acoustic ducting of the cryocooler itself has a nominal inner radius of about 11 mm with some deliberate variations along the path.

In Figure 4a, the acoustic power is plotted. The first black segment corresponds to power added by the driven diaphragm flexures. The compression side ducting transfers this power with low loss to the regenerator (cyan segment where the acoustic power drops). The ambient temperature heat exchanger is the short black segment to the left of the regenerator. To the right of the regenerator, the magenta segment is the vaned diffuser cone that rapidly reduces the duct diameter up to the venturi segment. The venturi segment is to the right of the diffuser, with its location indicated by the dashed line. The power diverted into the SCL loop is modelled as a pair of side branch impedances, but the change in power is too small to be readily visible. The cyan segment to the right of the venturi is the buffer tube, where the working gas gradually returns to ambient temperature.

The apparatus's 77K section is between the cyan regenerator segment and the cyan buffer tube segment, and includes the SCL components, which do not appear in this figure. Residual acoustic power (≈0.4 kW) is returned to the driver and absorbed by the flexure motion in the blue segment at the right end.

The total cooling power is the difference between acoustic power out of the cold side of the regenerator and the total power flow in the regenerator from the ambient side to the cold side [11].

$$\dot{Q}_{tot} = P_{ac} - P_{tot} \tag{3}$$

However, the net cooling power is less due to heat leakage into the cold zone $\dot{Q}_k$ by conduction, convection, or radiation, heat transport down the buffer tube $\dot{Q}_b$, and any power dissipated $P_{dis} + P_{SCL}$ in the cold zone (dashed blue box in Figure 1). For comparison purposes the extended loop dissipation P_{SCL} is separated from the trunk flow losses P_{dis}.

$$\dot{Q}_{net} = \dot{Q}_{tot} - \dot{Q}_k - \dot{Q}_b - P_{dis} - P_{SCL} \tag{4}$$

The cryocooler is assumed to be vacuum insulated and radiation-shielded. Then the parasitic conduction overhead $\dot{Q}_k$ is only the thermal conduction in the regenerator sleeves and the buffer tube wall. The regenerator sleeves may be constructed from very high strength and relatively low thermal conductivity material such as Inconel 718 to minimize sleeve wall thickness and thermal conduction.

Table 1. Simulated Powers (W)

P_{ac}	P_{tot}	$\dot{Q}_k$	$\dot{Q}_b$	P_{dis}	P_{SCL}	$\dot{Q}_{tot}$	$\dot{Q}_{net}$
445.6	132.0	13.2	12.9	41.7	8.3	313.6	237.5

The thermoacoustic simulation calculates the acoustic and thermal powers based on model dimensions and other inputs. The dissipated power includes viscous losses, thermal hysteresis losses, local losses, and joint losses as calculated in all the cold segments [11]. The dissipated power also includes the acoustic power driving the self-circulating loop and the steady flow dissipation through the cooling loop, as this is all dissipated in the cold zone. The simulation results for the quantities in Equations 3 and 4 are displayed in Table 1.

The net simulated cooling power is about 0.24 kW with an acoustic input power of 2.3 kW. As 0.4 kW is returned to the driver, the net drive required is 1.9 kW, resulting in a simulated COP of 0.12. With rolled foil regenerators, the result was a bit worse at 208 W net cooling with a COP of 0.11, primarily due to higher total power in the regenerator. With random wire felt regenerators, the result was 140 W of cooling and a COP of 0.06.

The expansion manifold of Figure 1 has a mass of 0.63 kg. The summed mass of the TA ducting, the regenerators, and the cold heat exchangers is 2.45 kg. The SCL ducting is another 1.4 kg, while the existing driver is 30 kg. The total system mass is about 34 kg, assuming all stainless steel and copper construction. With 230 W of cooling, this is a specific cooling power of 6.8 W/kg. The acoustic driver dominates the system mass, but not much effort has yet gone into reducing the driver mass. A new driver concept has a tentative mass estimate under 10 kg even with mostly steel construction, but it still requires much detailed design. With such a driver, the specific cooling power could be 17 W/kg. Even higher specific power would be possible by switching to lighter materials than steel but is then further from proven components and fabrication methods.

The total working gas volume is about 1.8 *l* but 0.95 *l* of that is in the cold zone of Figure 1 due to the substantial volume in the SCL ducting. A design operating pressure of 8 MPa would then result in an ambient temperature pressure of almost 20 MPa. Adding more volume at ambient temperature avoids designing the ducting and driver for this substantially higher pressure. The additional volume can be a separate small pressure vessel connected to the expansion volume of the acoustic driver where the pressure amplitude is low (right end of Figure 4). The same quarter wavelength tuned duct principle as in the SCL is applicable [6]. Only a capillary tuned connecting duct is required as the pressure equalization flow rates while the apparatus is cooling down or heating up are very small. The combination of small pressure amplitude in the driver expansion volume and the tiny connecting duct diameter means that acoustic losses from this addition are negligible.

Not included in the calculation is a heat transport contribution from any unwanted secondary flows in the regenerators or the buffer tube. The secondary flows are assumed to be non-existent. Secondary flows are far more detrimental to cryocooler performance than engine performance and are inherently more likely in coolers than engines [15]. To avoid driving secondary flows, the design must keep all the flows as symmetrical as possible. Regenerator uniformity must also be excellent [16]. Demonstrating an engine built with the same fundamental components and with negligible secondary flows [12] is not enough to guarantee that this will also be the case for a cryocooler. The actual achievable secondary flow suppression with this hardware in a cryocooler application is currently unknown and is the only substantial risk factor in successfully implementing this design.

CONCLUSIONS

The simulation of a high-frequency regenerative cryocooler using an SCL to cool an extended area indicates that the proposed approach is auspicious. Such a cryocooler would achieve the functionality of hybrid systems currently used for distributed cooling at a much lower cost as the extra components that enable the self-circulation are nothing more than tubing.

A system with extended area cooling might be lower cost than the equivalent system with an expansion heat exchanger and only point cooling capability, as the ultra-compact heat exchanger then required pushes the manufacturing state of the art and is much more complicated than tubing. Furthermore, the performance of the extended area cooling version is better than the point cooling version, as the SCL losses are less than expansion exchanger losses with all else equal.

Adding an SCL-driven extended area cooling loop to a previously proposed looped thermoacoustic cryocooler enhances its functionality, performance, and cost. If implemented, it is highly likely to become a favored option for many applications that require extended area cooling and even for those that do not. The system's simplicity and the components' inherent design mean it can be ultra-reliable. The only implementation risk is that secondary flows in the regenerator and buffer tube cannot be sufficiently engineered away and decrease the performance to unacceptable levels.

REFERENCES

1. Radebaugh, R., "Cryocoolers: the state of the art and recent developments," *J. Phys.: Condensed Matter*, 21 (2009) 164219.
2. Petach, M.B., Amouzegar, L.A., "Cryocooler with novel circulator providing broad area cooling at 90 K for spaceflight applications," *Cryocoolers 21*, ICC Press, Boulder Colorado, USA, (2021), pp. 115–124.
3. Frank, D., Ruiz, D.A., Guzinski, M., Roth, E., Mistry, V., Yengoyan, H., Olson, J., "Space Cryogenic Circulator," *Cryocoolers 21*, ICC Press, Boulder Colorado, USA, (2021), pp. 107–113.
4. Steiner, T.W., "High-frequency, steel-flexure, acoustic-to-electric transducer for cryocoolers," *Cryocoolers 21*, ICC Press, Boulder Colorado, USA, (2021), pp. 337-345.
5. Swift, G.W., Backhaus, S., "A resonant, self-pumped, circulating thermoacoustic heat exchanger," *J. Acoust. Soc. Am.* 116 (2004) 2923–2938.
6. Steiner, T.W., "Thermoacoustic transducer apparatus including a working volume and reservoir volume in fluid communication through a conduit," US patent 11,041,458 (2021).
7. Elferink, M., Steiner, T., "Thermoacoustic waste heat recovery engine, Comparison of simulation and experiment," *Proc. Mtgs. Acoust.* 35, (2018) 065002. doi:https://doi.org/10.1121/2.0000978.
8. Kotsubo, V. "Real and reactive flows in regenerative cryocoolers," *Cryocoolers 21*, ICC Press, Boulder Colorado, USA, (2021), pp. 245-253.
9. Idelchik, I.E. *Handbook of Hydraulic Resistance*, 3rd Edition, Jaico, Mumbai, India, (2003).
10. Landau, L.D., Lifshitz, E.M., *Fluid Mechanics*, Pergamon Press, Oxford, UK, (1982).
11. Swift, G.W., *Thermoacoustics A Unifying Perspective for Some Engines and Refrigerators*, 2nd Edition, ASA Press/Springer, Cham, Switzerland, (2017).
12. Steiner, T.W., Hoy, M., Antonelli, K.B., Malekian, M., Archibald, G.D.S., Kanemaru, T., Aitchison, W., De Chardon, B., Gottfried, K.T., Elferink, M., Henthorne, T., O'Rourke, B., Kostka, P., "High-efficiency natural gas fired 1 kWe thermoacoustic engine," *Appl. Therm. Eng.* 199 (2021) 117548. doi:https://doi.org/10.1016/j.applthermaleng.2021.117548.
13. Steiner, T.W., Antonelli, K.B., Archibald, G.D.S., de Chardon, B., Gottfried, K.T., Malekian, M., Kostka, P. "A high frequency, power, and efficiency diaphragm acoustic-to-electric transducer for thermoacoustic engines and refrigerators," *J. Acoust. Soc. Am.* 149 (2021) pp. 948–959. doi:https://doi.org/10.1121/10.0003495.
14. Steiner, T.W., Hoy, M.P., Archibald, G.D.S., Gottfried, K.T., Kanemaru, T., Medard de Chardon, B., "Apparatus and system for exchanging heat with a fluid," US patent 10,890,385 (2019).
15. So, J.H., Swift, G.W., Backhaus, S., "An internal streaming instability in regenerators," *J. Acoust. Soc. Am*. 120 (2006) pp. 1898–1909.
16. Gedeon, D., "Flow circulation in foil-type regenerators produced by nonuniform layer spacing," *Cryocoolers 13*, Springer, New York, USA, (1999), pp. 421–430.